Calorimetric quantification of linked equilibria in cyclodextrin/lipid/detergent mixtures for membrane–protein reconstitution

ARTICLE *in* METHODS · JANUARY 2015

Impact Factor: 3.65 · DOI: 10.1016/j.ymeth.2015.01.002 · Source: PubMed

3 AUTHORS, INCLUDING:

Sandro Keller
Technische Universität Kaiserslautern
89 PUBLICATIONS **1,298** CITATIONS

SEE PROFILE

Methods 76 (2015) 183–193

Contents lists available at ScienceDirect

Methods

journal homepage: www.elsevier.com/locate/ymeth

Calorimetric quantification of linked equilibria in cyclodextrin/lipid/detergent mixtures for membrane-protein reconstitution ☆

Martin Textor, Carolyn Vargas, Sandro Keller *

Molecular Biophysics, University of Kaiserslautern, Erwin-Schrödinger-Str. 13, 67663 Kaiserslautern, Germany

ARTICLE INFO

Article history:
Received 30 November 2014
Received in revised form 30 December 2014
Accepted 2 January 2015
Available online 10 January 2015

Keywords:
Isothermal titration calorimetry
Detergent removal
Phase diagram
Vesicles
Micelles
Mistic

ABSTRACT

Reconstitution from detergent micelles into lipid bilayer membranes is a prerequisite for many in vitro studies on purified membrane proteins. Complexation by cyclodextrins offers an efficient and tightly controllable way of removing detergents for membrane-protein reconstitution, since cyclodextrins sequester detergents at defined stoichiometries and with tuneable affinities. To fully exploit the potential advantages of cyclodextrin for membrane-protein reconstitution, we establish a quantitative model for predicting the supramolecular transition from mixed micelles to vesicles during cyclodextrin-mediated detergent extraction. The model is based on a set of linked equilibria among all pseudophases present in the course of the reconstitution process. Various isothermal titration-calorimetric protocols are used for quantifying a detergent's self-association as well as its colloidal and stoichiometric interactions with lipid and cyclodextrin, respectively. The detergent's critical micellar concentration, the phase boundaries in the lipid/detergent phase diagram, and the dissociation constant of the cyclodextrin/detergent complex thus obtained provide all thermodynamic parameters necessary for a quantitative prediction of the transition from micelles to bilayer membranes during cyclodextrin-driven reconstitution. This is exemplified and validated by stepwise complexation of the detergent lauryldimethylamine *N*-oxide in mixtures with the phospholipid 1-palmitoyl-2-oleoyl-*sn*-glycero-3-phosphocholine upon titration with 2-hydroxypropyl-β-cyclodextrin, both in the presence and in the absence of the membrane protein Mistic. The calorimetric approach presented herein quantitatively predicts the onset and completion of the reconstitution process, thus obviating cumbersome trial-and-error efforts and facilitating the rational optimisation of reconstitution protocols, and can be adapted to different cyclodextrin/lipid/detergent combinations.

1. Introduction

A better understanding of membrane proteins is of utmost importance for both basic and pharmaceutical research [1]. However, membrane proteins such as channels or transporters need to reside within a lipid bilayer to exert their native activities and be amenable to functional assays [2]. Hence, such membrane proteins have to be reconstituted after their detergent-mediated solubilisation and purification by transfer from a micellar environment into a lipid bilayer [3]. Membrane-protein reconstitution is often achieved by solubilising a purified protein along with lipids of choice in a suitable detergent and then decreasing the detergent concentration in this ternary protein/lipid/detergent mixture to a value sufficiently low to allow for the spontaneous formation of proteoliposomes. During this process, the protein, the lipid, and some residual detergent are transferred from mixed micelles into mixed bilayers, which usually assume the form of vesicles. These supramolecular structures, as well as the bulk aqueous solution containing detergent monomers, can—from a thermodynamic viewpoint and to a first approximation—be treated as pseudophases [4].

The phase diagram for a given lipid/detergent pair provides the concentrations at which the transitions between the different pseudophases occur in the absence of protein (Fig. 1A). In the simplest case, which is a good approximation for many lipid/detergent combinations [4–6], these phase boundaries are straight lines defined by slopes $R_D^{b,SAT}$ and $R_D^{m,SOL}$ and a common ordinate intercept $c_D^{aq,\circ}$. The latter denotes the concentration of detergent monomers in the aqueous phase, which is constant within the micelle/vesicle coexistence range separating the purely micellar from the purely vesicular range of the phase diagram. Before reconstitution, the sample is in the micellar range, where only mixed micelles are

☆ *Note:* The authors declare no competing financial interest.

* Corresponding author. Fax: +49 631 205 4895.
E-mail address: mail@sandrokeller.com (S. Keller).

http://dx.doi.org/10.1016/j.ymeth.2015.01.002
1046-2023/

present. Upon detergent removal, vesicle formation sets in when the solubilisation (SOL) boundary is crossed. Within the coexistence range, both mixed micelles and mixed vesicles are present in the suspension. Eventually, the saturation (SAT) boundary is reached, beyond which only mixed vesicles persist. Further detergent removal may bring the detergent concentration below its critical micelle concentration (CMC). However, it should be noted that the vesicular range of the phase diagram encompasses a region where only mixed vesicles exist even though the total detergent concentration is above the CMC, because the detergent is not only present in the aqueous phase but rather partitions between the latter and the bilayer phase.

To induce a transition from micelles to vesicles for membrane-protein reconstitution, several strategies have been established, including (i) dilution, (ii) dialysis, (iii) gel filtration, (iv) adsorption to bio-beads, and (v) complexation by cyclic oligosaccharides called cyclodextrins (CDs) [3,7,8]. These methods substantially differ from one another with respect to their capability of controlling the rate at which detergent is removed from the reconstitution mixture. Besides the properties of the detergent itself, in particular, its ability to equilibrate across the bilayer on the experimental timescale [9], the rate of detergent extraction affects the size of the vesicles formed during the reconstitution process. Slow rates usually lead to larger vesicles and allow homogeneous reconstitution, whereas faster rates lead to smaller vesicles and might fare better at preventing protein aggregation [3,10,11]. Combinations of several of the above methods can enable better control of vesicle size [12].

(i) Dilution is well suited for detergents having high CMCs [11,13], and stepwise addition of dilution buffer allows for controlling the rate of reconstitution. However, residual detergent is present after dilution and has to be removed by other means, and concomitant dilution of protein and lipid is inevitable (Fig. 1A). (ii) Dialysis is a common method for membrane-protein reconstitution, which, to a certain extent, enables control of the rate of detergent removal provided a continuous flow-through dialysis apparatus is used [14,15]. However, dialysis requires long durations for low-CMC detergents, which can pose problems for less stable membrane proteins. (iii) Gel filtration, although less commonly used for reconstitution, allows for efficient detergent removal [16] but holds the drawback of considerable retention of lipid on the column matrix [17] and, moreover, hardly allows for rate control. (iv) By contrast, hydrophobic adsorption of detergent onto polystyrene beads known as bio-beads is a widely used strategy for detergent removal in reconstitution protocols and 2D crystallisation [18–20]. The kinetics of detergent adsorption onto bio-beads has been systematically studied by Rigaud and coworkers [19]; accordingly, the rate of detergent extraction can be controlled by varying the amount of beads added to the protein/lipid/detergent mixture. Nevertheless, using very small amounts of beads to achieve slow rates can be difficult [17]. Moreover, although the adsorptive capacity of bio-beads for egg yolk phosphatidylcholine is two orders of magnitude lower than that for detergents [19], significant lipid adsorption cannot be excluded a priori for other phospholipids. (v) Complexation by CDs has been introduced as an alternative method for sequestering detergents to promote micelle-to-vesicle transitions for membrane-protein reconstitution [21].

The oligosaccharide rings of α-, β-, and γ-CDs consist of 6, 7, or 8 α-D-glucopyranoside units, respectively (Fig. 1B). The glycosidic oxygen bridge and the hydrogens of carbon atoms 3 and 5 of each glucopyranose unit line the nonpolar cavity of the conically shaped CD ring, which can bind small hydrophobic molecules such as cholesterol and detergent alkyl chains. The hydroxyl groups of the glucopyranose units lie on the exterior of the ring and thus confer solubility in polar solvents. Randomly methylated β-cyclodextrin

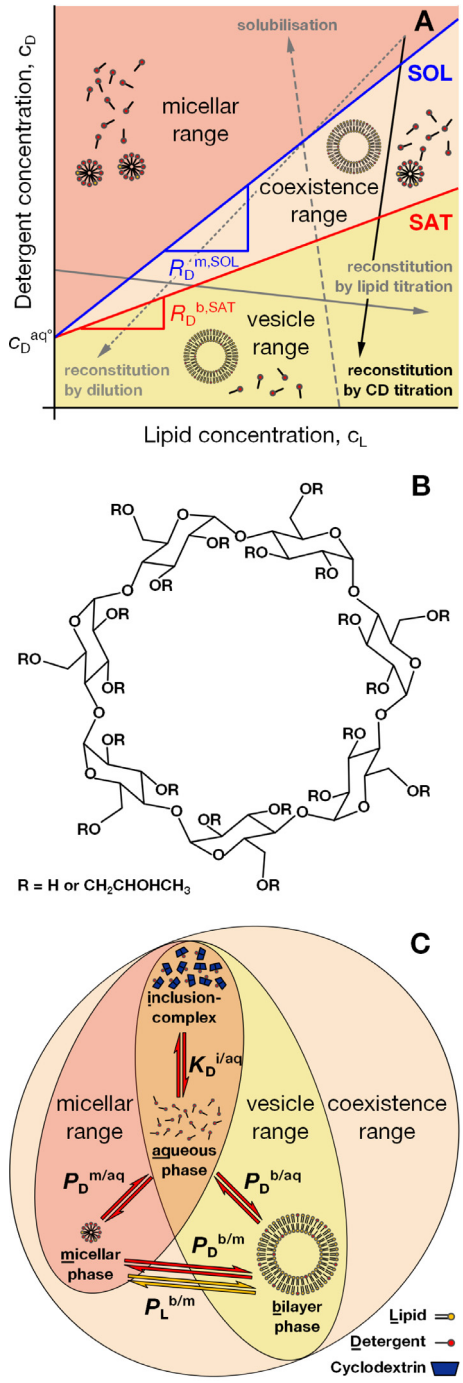

Fig. 1. Lipid/detergent phase diagram, chemical structure of cyclodextrin, and linked equilibria in a ternary cyclodextrin/lipid/detergent mixture. (A) Representative lipid/detergent phase diagram with solubilisation (SOL) and saturation (SAT) boundaries, which are defined by their slopes $R_D^{m,SOL}$ and $R_D^{b,SAT}$, respectively, and their common ordinate intercept $c_D^{aq^\circ}$. Arrows denote exemplary trajectories of different experiments involving transitions between pseudophase ranges, including solubilisation and reconstitution by dilution, addition of lipid, or extraction of detergent with the aid of cyclodextrin. (B) Chemical structure of 2-hydroxypropyl-β-cyclodextrin. The average molar degree of substitution of the derivative used in this study was 1.0; thus, on average, each glucopyranose unit carried one 2-hydroxypropyl substituent. (C) Linked equilibria in a ternary cyclodextrin/lipid/detergent mixture as described by the partition coefficients P_L and P_D for the lipid (yellow arrows) and the detergent (red arrows), respectively, and by the dissociation constant $K_D^{i/aq}$ of the cyclodextrin/detergent complex.

(MβCD) is a derivative that is frequently used for the removal of cholesterol from lipid bilayers [22] and also has allowed for successful 2D crystallisation [23]. Other hydroxyl group substitutions

grant access to a plethora of additional CD derivatives such as 2-hydroxypropyl-β-cyclodextrin (HPβCD; Fig. 1B), which considerably differ in their physicochemical properties, in particular, with respect to water solubility and ligand specificity [24]. The use of CDs for detergent removal overcomes many of the limitations associated with the more conventional techniques described above. CDs sequester detergents of both low and high CMCs without loss of sample or substantial dilution. Since most CDs do not significantly absorb in the ultraviolet and visible wavelength range, the reconstitution process can be monitored in solution by spectroscopic methods [25], and reconstitution trials can be downscaled to even lower sample volumes as compared with bio-beads [19]. Additionally, stepwise addition of CD, in conjunction with stoichiometric detergent binding, permits accurate rate control and virtually complete removal of detergent at sufficiently high CD concentrations.

However, to fully exploit the potential advantages of CD-driven membrane-protein reconstitution, a quantitative model that is able to predict the supramolecular state in a complex protein/CD/lipid/detergent mixture and the phase transitions encountered during a reconstitution titration is desirable. To this end, it is imperative to obtain a thorough quantification of all relevant linked equilibria (Fig. 1C), which are described by a set of partition coefficients between each two of the pseudophases involved and by the dissociation constant of the CD/detergent complex. For a given set of CD, lipid, and detergent, all of these parameters can be conveniently determined by isothermal titration calorimetry (ITC) using a range of established protocols. (i) The partitioning of detergent (D) between the micellar (m) phase and the aqueous (aq) phase, $P_D^{m/aq}$, is related to and thus given by the CMC (Eq. (1), Section 6), which can be determined in a demicellisation experiment by titrating detergent micelles into buffer (Section 3.1) [26]. The resulting isotherm typically has a sigmoidal shape, and the detergent concentration at the inflection point in the transition region is taken as the CMC. (ii) The partition coefficients of detergent and lipid (L) between the micellar phase and the bilayer (b) phase, $P_D^{b/m}$ and $P_L^{b/m}$, respectively, are derived from the lipid/detergent phase diagram (Section 3.2). The latter is obtained from a series of solubilisation and reconstitution experiments, where detergent is titrated to lipid vesicles or vice versa, respectively [5,25]. In reconstitution isotherms, the first and second inflection points indicate the SOL and SAT boundaries, respectively. In solubilisation titrations, by contrast, the SAT boundary is reached before the SOL boundary. The detergent concentrations at the inflection points of the isotherms are plotted against the corresponding lipid concentrations to obtain the SAT and SOL boundaries in the phase diagram, which usually can be fitted by straight lines (Eqs. (3) and (4)). The detergent's CMC obtained from the above demicellisation experiment can be used to determine the ordinate intercept of the phase boundaries (Eq. (15)) and thus reduce the number of adjustable parameters. (iii) Finally, the dissociation constant of the CD/detergent inclusion complex (i), $K_D^{i/aq}$, is derived from a conventional ITC binding experiment in which a detergent solution below the CMC is titrated with CD (Section 3.3) [24,27].

By combining the thermodynamic parameters describing the above linked equilibria in ternary CD/lipid/detergent mixtures, we have devised a quantitative model that allows determination and prediction of the supramolecular state in a reconstitution mixture as a function of CD concentration (Section 3.4). We have tested the model for prediction of the phase transitions observed during CD-driven detergent extraction in a mixture of the zwitterionic detergent lauryldimethylamine *N*-oxide (LDAO) and the zwitterionic phospholipid 1-palmitoyl-2-oleoyl-*sn*-glycero-3-phosphocholine (POPC). To demonstrate the applicability of the approach to membrane-protein reconstitution, we have applied it to the CD-mediated reconstitution of the membrane protein Mistic [28] from LDAO micelles into POPC vesicles. The quantitative model facilitates the design of reconstitution protocols and, in combination with a comprehensive calorimetric approach, allows for a quick, rational, and directed optimisation of key experimental parameters such as the protein/lipid ratio and the rate of detergent removal.

2. Experimental section

2.1. Materials and sample preparation

POPC was obtained from Lipoid (Ludwigshafen, Germany), and LDAO and HPβCD (average molar degree of substitution 1.0) were purchased from Sigma–Aldrich (Steinheim, Germany). NaCl was from VWR (Darmstadt, Germany), and Tris-(hydroxymethyl)-aminomethane (Tris) and 1,4-dithiothreitol (DTT) were from Roth (Karlsruhe, Germany). All experiments were performed in 50 mM Tris buffer containing 50 mM NaCl and adjusted to pH 7.4. Large unilamellar vesicles composed of POPC for solubilisation and reconstitution experiments were prepared by 35 extrusion steps through two stacked polycarbonate filters with a pore diameter of 100 nm using a LiposoFast extruder (Avestin, Ottawa, Canada). Mistic [28] was produced and purified as described elsewhere [29], and reconstitution mixtures were freshly supplemented with 5 mM DTT to prevent protein dimerisation [30].

2.2. Isothermal titration calorimetry

Calorimetric titrations for deriving thermodynamic parameters were performed on a VP-ITC (Malvern Instruments, Worcestershire, UK). These experiments included: (i) LDAO demicellisation for CMC determination, where 26 mM LDAO was titrated into buffer. (ii) Solubilisation and reconstitution experiments yielding the POPC/LDAO phase diagram. For solubilisation, 30 mM, 65.5 mM, 85 mM, or 131 mM LDAO was titrated to 1 mM, 3 mM, 4.5 mM, or 6 mM POPC vesicles, respectively. For reconstitution, 15 mM, 15 mM, 35 mM, or 40 mM POPC vesicles were titrated to 4 mM, 6 mM, 9 mM, or 13 mM LDAO, respectively. (iii) A binding experiment for determination of the dissociation constant of the HPβCD/LDAO complex, in which 10 mM HPβCD was titrated into 1 mM LDAO. For all of these experiments, the injection volume was set to 4 μL, the time spacing to 900 s, the stirrer speed to 310 rpm, the filter period to 2 s, and the reference power to 75 μJ/s. Validation of the model by stepwise detergent extraction with HPβCD from a POPC/LDAO mixture was performed by titrating 75 mM HPβCD into a mixture of 3 mM POPC and 12 mM LDAO using the same instrumental settings. Mistic reconstitution was monitored on an ITC_{200} (Malvern Instruments) at a protein/lipid molar ratio of 1:200. To this end, 149.3 mM HPβCD was progressively added to a ternary mixture of 70 μM Mistic, 14 mM POPC, and 40 mM LDAO using an injection volume of 0.4 μL, a time spacing of 120 s, a stirrer speed of 1000 rpm, a filter period of 5 s, and a reference power of 25 μJ/s. The protein concentration was chosen to allow a good signal/noise ratio in subsequent circular dichroism experiments. All ITC measurements were carried out at 25 °C.

For analysis of raw thermograms, automated baseline assignment by singular value decomposition and peak integration were performed using NITPIC [31]. The CMC of LDAO was derived from a demicellisation isotherm fitted with a generic sigmoidal function according to Eq. (2) [32]. SAT and SOL boundaries in the phase diagram were taken from global linear fits according to Eqs. (3) and (4) to the lipid and detergent concentrations corresponding to local minima and maxima in the first derivatives within the transition regions of solubilisation and reconstitution isotherms [33]. The dissociation constant of the HPβCD/LDAO complex was determined by

nonlinear least-squares fitting of the binding isotherm in SEDPHAT with a one-site binding model [34]. The precision of parameters obtained by fits to demicellisation and binding experiments was evaluated in terms of the width of the corresponding 95% confidence intervals as detailed elsewhere [35]. Error margins for phase diagram parameters and predicted phase boundaries were derived by fitting the phase boundaries individually to either solubilisation or reconstitution data, because the systematic deviations between these two types of experiments were larger than the stochastic errors within each type of experiment.

2.3. Dynamic light scattering and circular dichroism spectroscopy

Particle size distributions before and after reconstitution were assessed by dynamic light scattering (DLS) on a Zetasizer Nano S90 (Malvern Instruments) equipped with a 633-nm He–Ne laser and operating at a detection angle of 90°. Measurements were carried out in a 3 mm × 3 mm quartz glass cuvette (Hellma Analytics, Müllheim, Germany) using automatically determined attenuator positions. The influence of all buffer components on viscosity and refractive index were accounted for during data analysis, which was carried out by fitting the experimentally determined autocorrelation function with a non-negatively constrained least-squares function [36] to yield the size distribution in terms of the mean percentage of scattering intensity as a function of particle size. The secondary structure of Mistic before and after reconstitution was analysed by far-UV circular dichroism spectroscopy on a Chirascan-plus circular dichroism spectrometer (Applied Photophysics, Leatherhead, UK). The cuvette used had a pathlength of 0.2 mm (Hellma Analytics), and experimental parameters were set to a digital integration time of 1 s, a bandwidth of 1 nm, and a step size of 1 nm. A buffer blank was subtracted from the average of five spectra, and the resulting spectrum was offset-corrected by subtracting the average ellipticity in the range of 270–280 nm and normalised to mean residue molar ellipticity (θ, given in k° cm^2 dmol^{-1}).

3. Results

The thermodynamic model presented herein enables a quantitative prediction of the phase transitions encountered during CD-mediated membrane-protein reconstitution. We used a ternary mixture of HPβCD, POPC, and LDAO as a representative example of the practical application of the approach. For this system, the CMC, $R_D^{b,SAT}$, $R_D^{m,SOL}$, and $K_D^{i/aq}$ values at 25 °C were determined by ITC, and the model was validated by comparison of the predicted phase boundaries with those observed in calorimetrically monitored reconstitution titrations, both in the absence and in the presence of the membrane protein Mistic.

3.1. LDAO demicellisation

The CMC of LDAO was derived from a demicellisation titration in which LDAO micelles were injected into buffer (Fig. 2). The sigmoidal shape of the isotherm thus obtained reflects the heat of demicellisation in the beginning, when the injected micelles dissociate into monomers, and the heat of dilution towards the end of the titration, when micelle disintegration has ceased at concentrations well above the CMC. From the inflection point of the isotherm, the CMC of LDAO was determined to be 1.94 mM (1.92–1.96 mM), and the molar micellisation enthalpy, derived from the difference between the pre- and post-transition baselines at the CMC, amounted to $\Delta H_D^{m/aq} = 7.9$ kJ/mol (7.2–8.5 kJ/mol) (Table 1).

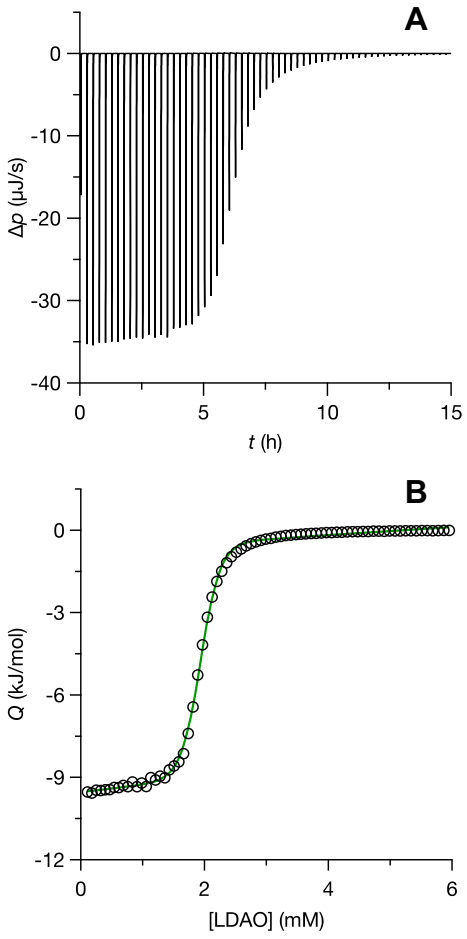

Fig. 2. Determination of the CMC of LDAO by ITC demicellisation at 25 °C. 26 mM LDAO was titrated into buffer (50 mM Tris, 50 mM NaCl, pH 7.4) in a series of 75 injections. (A) Raw thermogram depicting differential heating power, Δp, versus time, t. (B) Isotherm showing integrated and normalised heats of reaction, Q, versus LDAO concentration. Experimental data (circles) and generic sigmoidal fit (green solid line) according to Eq. (2), yielding a CMC of 1.94 mM, as derived from the LDAO concentration at the inflection point.

3.2. POPC/LDAO phase diagram

The POPC/LDAO phase diagram was obtained from a number of solubilisation and reconstitution experiments performed at different initial POPC and LDAO concentrations; two representative titrations are shown in Fig. 3. In the solubilisation experiment, micellar LDAO was titrated into a suspension of large unilamellar POPC vesicles having a diameter of ~170 nm (Fig. 3A). Initially, disintegration of micelles and transfer of LDAO monomers into the bilayer membrane were accompanied by net endothermic heats. An abrupt change at 8.9 mM LDAO to large exothermic heats marked the SAT boundary, which was followed by a plateau in the integrated heats (Fig. 3B) characteristic of the coexistence range. Within this range, the pseudophase model predicts that further addition of LDAO increases the number of mixed micelles at the expense of mixed vesicles without changing their compositions. At ~14.7 mM LDAO, the SOL boundary was reached, at which the last vesicles were solubilised. In the reconstitution experiment, POPC vesicles were titrated to LDAO micelles (Fig. 3C), so that the phase transitions showed up in reverse order as compared with the solubilisation experiment, that is, the SOL boundary at 2.4 mM POPC and the SAT boundary at 4.3 mM POPC (Fig. 3D). The POPC and LDAO concentrations corresponding to the SAT and SOL

Table 1
Thermodynamic parameter values derived from ITC experiments at 25 °C.

Experiment	Component C	p1 → p2	$E_C^{p2/p1}$	$\Delta G_C^{p2/p1,0}$ (kJ/mol)	$\Delta H_C^{p2/p1}$ (kJ/mol)	$-T\Delta S_C^{p2/p1,0}$(kJ/mol)
LDAO demicellisation	D	aq → m	28.6×10^3 (28.3×10^3 to 28.9×10^3)	−25.4 (−25.5 to −25.4)	7.88 (7.23 to 8.50)	−33.3 (−33.4 to −33.3)
POPC/LDAO phase diagram	D	aq → b	23.0×10^3 (22.8×10^3; 22.9×10^3)	−24.9 (−24.9; −24.9)		
	D	m → b	0.804 (0.796; 0.799)	0.541 (0.566; 0.556)		
	L	m → b	1.51 (1.52; 1.57)	−1.03 (−1.03; −1.12)		
LDAO/HPβCD binding	D	aq → i	103 μM (93.7 to 113 μM)	−22.8 (−23.0 to −22.5)	5.29 (5.18 to 5.41)	−28.1 (−28.3 to −27.8)

$E_C^{p2/p1}$ denotes an equilibrium constant. For the binding experiment, $E_C^{p2/p1}$ is the dissociation constant. For all other experiments, $E_C^{p2/p1}$ corresponds to the partition coefficient for the transfer of component C from pseudophase p1 to pseudophase p2. Standard molar Gibbs free energies, $\Delta G_C^{p2/p1,0}$, were calculated according to $\Delta G^0 = -RT\ln E_C^{p2/p1}$. The precision of parameter values derived from fits to demicellisation and binding experiments is expressed in terms of the width of 95% confidence intervals. Error margins for phase diagram parameters were derived from individual fits of the phase boundaries to either solubilisation or reconstitution data. Because of correlations between the ordinate intercept and the slopes of both the SAT and SOL boundaries, the values of the partition coefficients derived from only solubilisation or only reconstitution data do not bracket the best-fit value obtained from a simultaneous fit to all data.

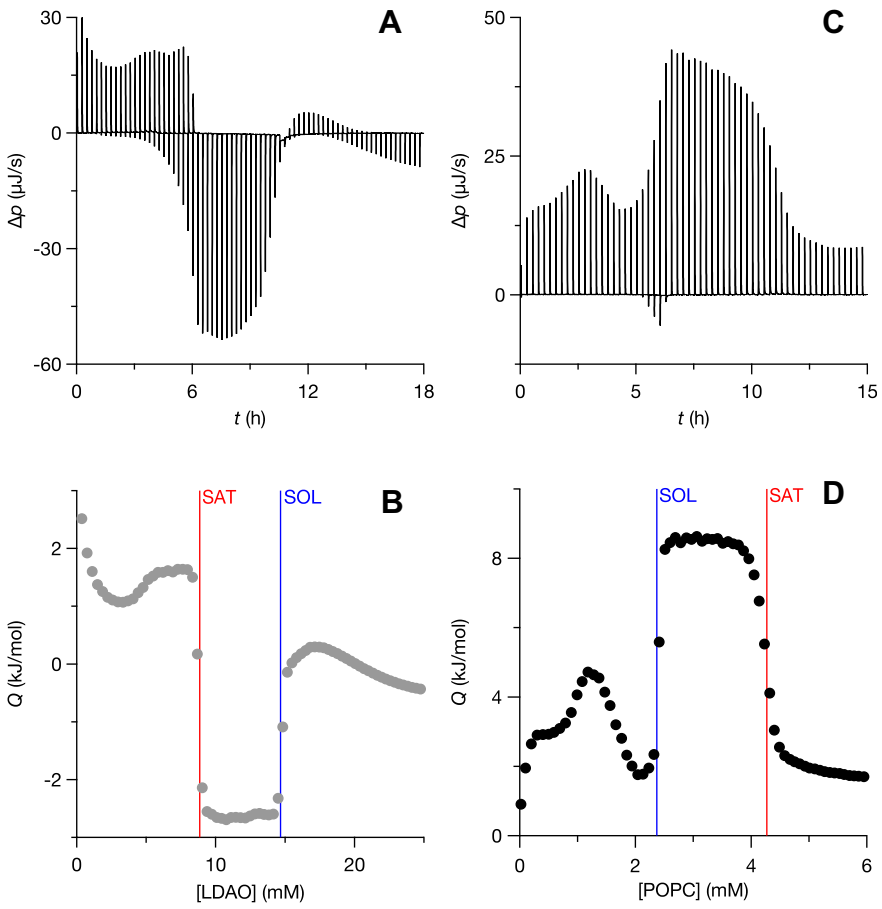

Fig. 3. LDAO-mediated solubilisation and reconstitution of POPC vesicles as monitored by ITC at 25 °C. (A, B) For solubilisation, 131 mM LDAO was titrated to 6 mM of POPC in the form of large unilamellar vesicles with an average diameter of ~170 nm in a series of 75 injections. (C, D) For reconstitution, 35 mM POPC vesicles were titrated to 9 mM LDAO in a series of 75 injections. (A, C) Raw thermograms showing differential heating power, Δp, versus time, t. (B, D) Isotherms depicting integrated and normalised heats of reaction, Q, versus titrant concentration. Experimental data (circles) and phase boundaries (vertical lines). Detergent and lipid concentrations corresponding to local minima and maxima in the first derivatives of isotherms were taken as SAT and SOL phase boundaries, respectively [5].

boundaries were extracted from the local minima and maxima, respectively, in the first derivatives within the transition regions.

A phase diagram was then constructed by plotting the LDAO concentrations at the SAT and SOL boundaries against the corresponding POPC concentrations and applying two linear fits with a shared ordinate intercept, $c_D^{aq^\circ}$ (Fig. 4). The latter was linked to $R_D^{m,SOL}$ through Eq. (15) by taking into account the CMC of LDAO determined above (Fig. 2). Error margins for the phase boundaries were estimated by fitting data from either solubilisation or reconstitution experiments individually. The fits yielded $R_D^{b,SAT} = 1.39$ (1.33–1.44) and $R_D^{m,SOL} = 2.62$ (2.53–2.83) for the slopes of the phase boundaries, with $c_D^{aq^\circ} = 1.40$ mM (1.39–1.43 mM) being the common ordinate intercept. From these values, the molar fractions of LDAO in detergent-saturated bilayers and in lipid-saturated micelles were calculated according to Eqs. (5) and (6) as $X_D^{b,SAT} = 0.58$ (0.57–0.59) and $X_D^{m,SOL} = 0.72$ (0.72–0.74), respectively.

3.3. Formation of HPβCD/LDAO inclusion complex

The dissociation constant, $K_D^{i/aq}$, characterising the stability of the inclusion complex formed by LDAO and HPβCD was

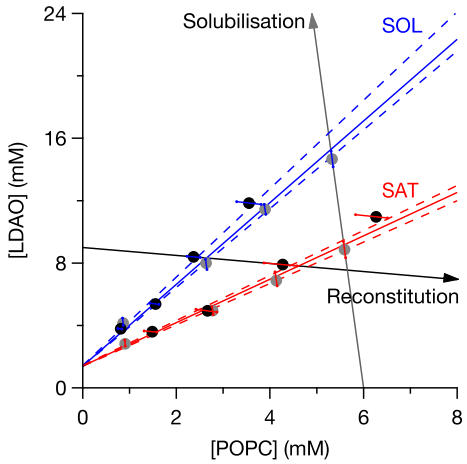

Fig. 4. POPC/LDAO phase diagram. Experimental data obtained by plotting LDAO concentrations against corresponding POPC concentrations at the inflection points showing up in solubilisation (grey circles) and reconstitution (black circles) titrations and linear fits to SAT and SOL boundaries (red and blue solid lines, respectively) with shared ordinate intercept. Uncertainties for individual data points (red and blue error margins) were derived from the widths of the transition regions in the corresponding isotherms, while uncertainties for phase boundaries (dashed lines) were estimated by fitting data from either solubilisation or reconstitution experiments alone. Arrows indicate the trajectories of the solubilisation and reconstitution experiments depicted in Fig. 3.

determined by a binding experiment (Fig. 5). By applying a one-site binding model to the experimental data, stoichiometric formation of a 1:1 inclusion complex of HPβCD and LDAO was confirmed, yielding $K_D^{i/aq} = 0.10$ mM (0.09–0.11 mM). Additional thermodynamic parameter values derived from all calorimetric experiments are summarised in Table 1.

3.4. Model validation

Following the establishment of all parameter values for the system at hand, the model was tested by comparing the phase transitions it predicted with those calorimetrically observed during CD-driven detergent extraction from a POPC/LDAO mixture (Fig. 6A). In this experiment, HPβCD was injected into mixed micelles composed of POPC and LDAO. The SOL and SAT boundaries were predicted to be reached at 2.8 mM and 6.2 mM HPβCD, respectively, which was in excellent agreement with the transitions observed experimentally (Fig. 6B). Moreover, we used the equilibrium constants compiled in Table 1 to calculate the concentrations of all species during the titration (Fig. 6C).

Finally, the model was employed for predicting the phase boundaries encountered in the course of the CD-mediated reconstitution of a membrane protein. Serving as a model protein, the 13-kDa four-helix bundle membrane protein Mistic [28] from *Bacillus subtilis* was reconstituted into POPC vesicles by stepwise addition of CD for gradual removal of LDAO, and the reconstitution process was monitored by ITC (Fig. 7A). To this end, HPβCD was titrated into a ternary, initially micellar reconstitution mixture composed of Mistic, POPC, and LDAO. The transitions in the resulting isotherm were less sharp than but still clearly reminiscent of those seen in the absence of protein (Fig. 6B). Within experimental error, the predicted phase boundaries coincide with the transition regions in the isotherm, implying that the presence of protein has no significant influence on the supramolecular state of the system and, thus, on the reconstitution process.

Successful reconstitution of Mistic was corroborated by DLS and circular dichroism spectroscopy. DLS revealed a unimodal size distribution and, thus, a uniform aggregational state both before and after reconstitution (Fig. 7B). Prior to reconstitution, a single peak

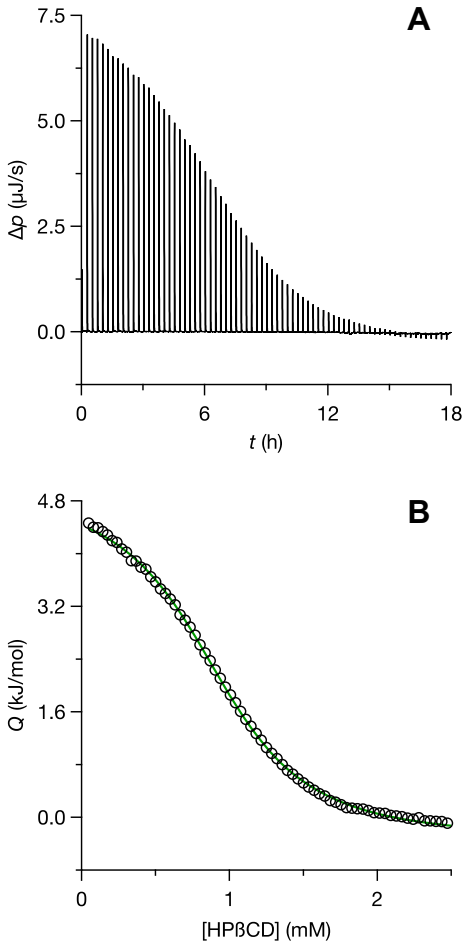

Fig. 5. Determination of $K_D^{i/aq}$ for the binding of LDAO to HPβCD by ITC at 25 °C. 10 mM HPβCD was titrated into 1 mM LDAO in a series of 75 injections. (A) Raw thermogram depicting differential heating power, Δ*p*, versus time, *t*. (B) Isotherm showing integrated and normalised heats of reaction, *Q*, versus HPβCD concentration. Experimental data (circles) and fit (green solid line) according to a one-site binding model, yielding $K_D^{i/aq}$ = 0.10 mM.

at an average hydrodynamic diameter of ~30 nm suggested the presence of rod-shaped protein/lipid/detergent micelles, as lipid-free Mistic/LDAO micelles are <10 nm in size [37]. After reconstitution, a pronounced shift to an average diameter of ~250 nm was evident, indicating the formation of large vesicles upon CD-mediated detergent removal. The mole fraction of residual detergent within these mixed vesicles was calculated to amount to $X_D^b = 0.56$ on the basis of the quantitative model. The circular dichroism spectrum of solubilised Mistic before reconstitution exhibited a double minimum at 208 nm and 222 nm characteristic of a largely α-helical conformation (Fig. 7C). The spectrum after reconstitution, corrected for the small dilution caused by addition of CD, superimposed virtually perfectly, demonstrating that no protein was lost as a result of aggregation or precipitation and that the secondary structure of Mistic was not affected by reconstitution.

4. Discussion

4.1. Combining different ITC protocols for predicting reconstitution trajectories

To quantify the parameters describing the linked equilibria for the particular CD/lipid/detergent system used, we first measured the CMC of LDAO, established the POPC/LDAO phase diagram, and

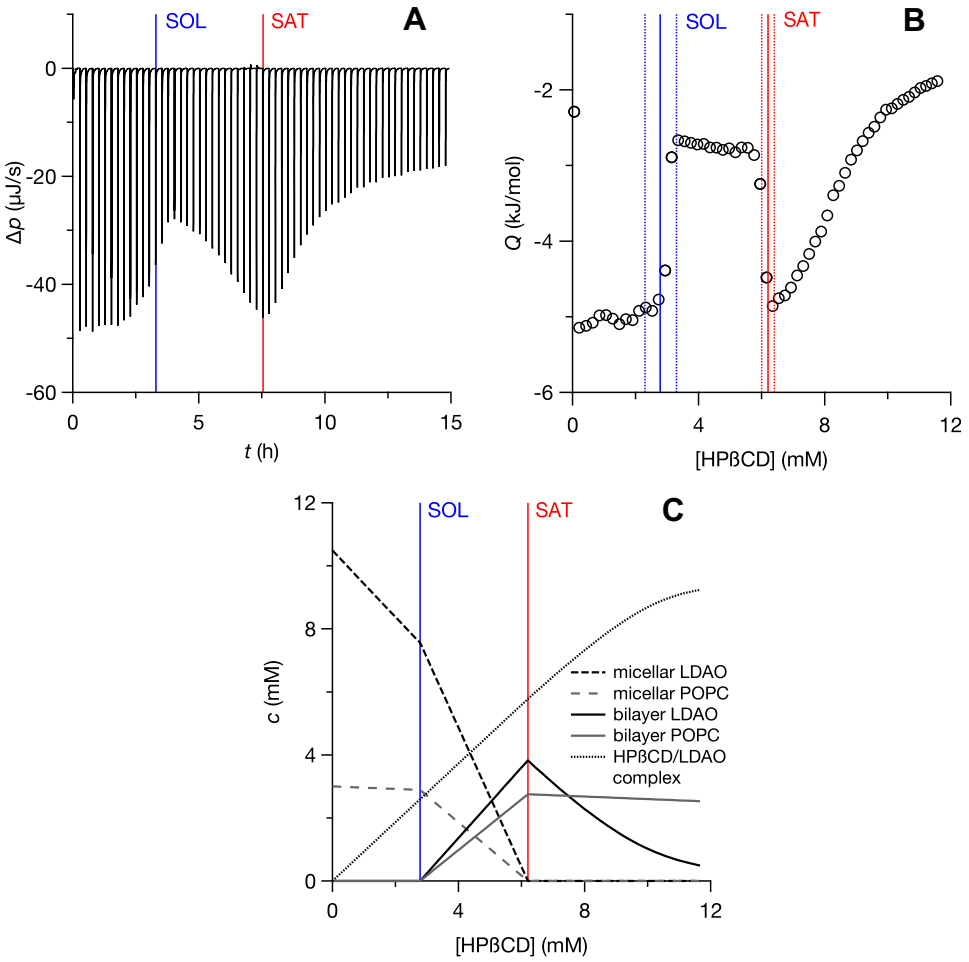

Fig. 6. CD-driven detergent extraction from mixed micelles by ITC at 25 °C. 75 mM HPβCD was titrated into a mixture of 3 mM POPC and 12 mM LDAO in a series of 60 injections. (A) Raw thermogram depicting differential heating power, Δp, versus time, t. (B) Integrated heats of reaction, Q, versus HPβCD concentration. SAT and SOL boundaries (solid lines) as predicted by the model are shown together with error margins (dotted lines). (C) Speciation plot derived from the model, illustrating the concentrations of POPC and LDAO in micelles and bilayers as well as the concentration of the HPβCD/LDAO inclusion complex in the course of the titration.

determined the dissociation constant of the HPβCD/LDAO inclusion complex. Based on these thermodynamic parameters, which were individually obtained from a range of diverse ITC protocols, the quantitative model presented herein allows for the prediction of the phase transitions occurring during CD-driven detergent extraction from reconstitution mixtures. Although all thermodynamic parameter values were derived from ITC experiments, it should be noted that these protocols greatly differ in terms of the rationale underlying their analysis. On the one hand, determination of $K_D^{i/aq}$ from conventional ITC binding titrations (Fig. 5) allows for, and actually requires, detailed modelling of the isotherm. On the other hand, solubilisation and reconstitution titrations (Fig. 3) with lipids and detergents involve rather complex processes even in the absence of CDs and membrane proteins. With a few exceptions representing particularly well-studied systems [38,39], such experiments therefore are amenable only to qualitative or, at best, semi-quantitative analysis [5]. Instead of a detailed fit of the entire isotherm, only the SAT and SOL boundaries are extracted from such titrations, which manifest themselves as sharp breakpoints in the isotherm. The partition coefficients of the lipid and the detergent become available only through a combination of several solubilisation and reconstitution experiments in a phase diagram (Fig. 4). Demicellisation titrations (Fig. 2) take an intermediate position between these two extremes; although they are usually not fitted on the basis of a physically meaningful model, the CMC can be obtained as the inflection point of a simple generic sigmoidal function [32]. Notwithstanding these fundamental differences, the above results demonstrate that the thermodynamic parameters individually retrieved from such conceptually diverse calorimetric protocols can be combined to furnish a quantitative picture of ternary mixtures of CD, lipid, and detergent (Fig. 6). The model even possesses predictive power for quaternary reconstitution mixtures additionally containing a membrane protein (Fig. 7), provided that the latter does not significantly affect the phase boundaries or introduce other complications [25].

4.2. Thermodynamic parameter values

A CMC of 1.94 mM is in agreement with literature values for LDAO under similar conditions [40,41]. The SAT and SOL boundaries of the phase diagram were derived from solubilisation and reconstitution experiments, the latter of which suggested slightly but systematically higher slopes for the phase boundaries than the solubilisation experiments (Fig. 4). In principle, hysteresis could account for discrepancies between solubilisation and reconstitution titrations [8]. However, this can be ruled out as a causal factor in the present case, because the inflection points in our solubilisation experiments, where detergent is added, occur at slightly lower detergent concentrations than in reconstitution

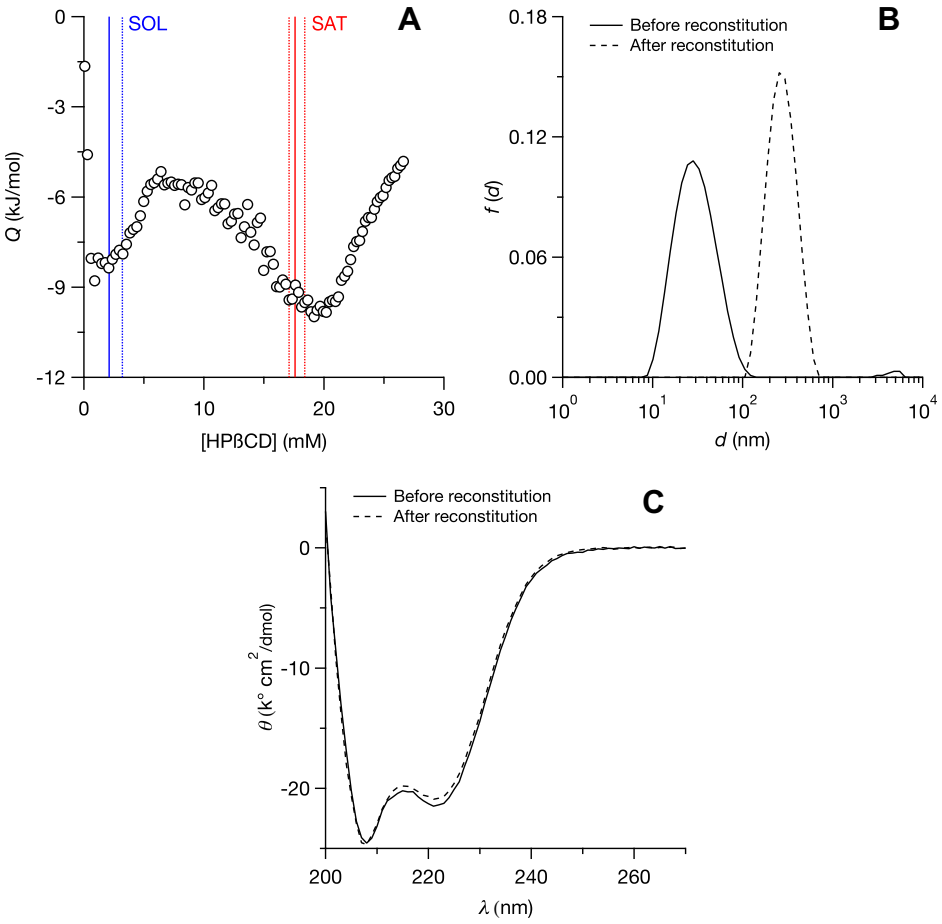

Fig. 7. CD-mediated reconstitution of Mistic into mixed POPC vesicles at 25 °C. (A) Integrated heats of reaction, *Q*, versus HPβCD concentration as monitored by ITC. 149 mM HPβCD was titrated into a ternary mixture of 70 μM Mistic, 14 mM POPC, and 40 mM LDAO in the presence of 5 mM DTT in a series of 100 injections. Phase boundaries predicted by the model (solid lines) are shown together with error margins (dotted lines). (B) Aggregational state before and after reconstitution as determined by DLS. Intensity-weighted size distribution function, $f(d)$, versus hydrodynamic diameter, d. (C) Confirmation of structural integrity of Mistic by circular dichroism spectroscopy. Normalised circular dichroism spectra before and after reconstitution are shown as mean residue molar ellipticity, θ, versus wavelength, λ.

experiments, where lipid is added. If hysteresis were an issue, the inflection points in solubilisation experiments would have been reached at higher detergent concentrations than in reconstitution experiments. Incomplete equilibration of LDAO across the membrane can also be excluded (see below). Notwithstanding these slight discrepancies, the phase boundaries and thermodynamic parameters derived from either solubilisation or reconstitution data are very similar to each other and to the values obtained from a simultaneous fit to all data (Table 1). The ordinate intercept of the phase diagram, $c_D^{aq^\circ} = 1.40$ mM, was considerably lower than the CMC, which is in accord with the pseudophase model underlying the quantitative analysis of the phase diagram (Fig. 4). Accordingly, $c_D^{aq^\circ}$ must be lower than the CMC because the latter refers to the partition equilibrium of detergent between the aqueous phase and pure detergent micelles, where $P_D^{m/aq} \equiv X_D^m/X_D^{aq} = 1/X_D^{aq} \approx 55.5\ \mathrm{M}/c_D^{aq}$ because $X_D^m = 1$. By contrast, $c_D^{aq^\circ}$ refers to the equilibrium between the aqueous phase and mixed lipid/detergent micelles, where $P_D^{m/aq} = X_D^{m,SOL}/X_D^{aq} \approx X_D^{m,SOL} \times 55.5\ \mathrm{M}/c_D^{aq^\circ}$ with $X_D^{m,SOL} < 1$. The dissociation constant of the HPβCD/LDAO complex, $K_D^{i/aq} = 0.10$ mM, is in a similar range as the values measured for the complexation by HPβCD of the cationic detergent dodecyltrimethylammonium chloride (0.18 mM) [42] and the nonionic detergent dodecyl-β-D-maltopyranoside (0.06 mM; Vargas et al., unpublished results). Like LDAO, both of these detergents bear a dodecyl chain, confirming that the stability of the inclusion complex is dominated by the length of the alkyl chain, whereas the polar headgroup has only a minor influence.

4.3. Experimental considerations

While the quantitative model presented herein may, in principle, apply to any CD/lipid/detergent mixture, some prerequisites have to be met for its successful implementation. First, the kinetics of detergent translocation between the two bilayer leaflets should be reasonably fast to allow for complete equilibration after each injection in both solubilisation and reconstitution titrations [9,39]. If necessary, this requirement can be confirmed, again with the aid of ITC, by so-called uptake and release experiments [43]. Such experiments indicate rapid equilibration of LDAO across POPC bilayers as reflected in a lipid accessibility factor of $\gamma = 1$ (Textor et al., unpublished results). Second, a suitable CD derivative has to be chosen that is sufficiently soluble, because the titrant concentration limits the concentration of detergent that can be complexed and thus extracted from the reconstitution mixture. Additionally, it has to be ensured that the CD derivative complexes the detergent used but not the lipid. For example, POPC is solubilised by MβCD [44], and we have observed significant complexation of 1,2-dilauroyl-*sn*-glycero-3-phosphocholine (DLPC) by HPβCD (Textor et al., unpublished results). The latter lipid has a short alkyl chain and, thus, is more prone to formation of an inclusion complex with CD.

Proteoliposomes formed during reconstitution titrations such as the one exemplified above reproducibly reveal an average hydrodynamic diameter of 200–300 nm (Fig. 7B). This relatively large size is due to the presence of residual zwitterionic detergent (X_D^b = 0.56) with high fusogenic activity [45] and the slow rate of detergent removal [10] and, thus, may be tuned by changing the final CD concentration or the rate of CD addition. While CD-mediated reconstitution starting from the micellar range is possible as demonstrated, one might also consider a different approach based on the addition of detergent-solubilised membrane protein to a mixture of CD and preformed vesicles for a tighter control of vesicle size. With the model at hand, reconstitutions starting from different regions of the phase diagram may be set up to promote asymmetric reconstitution aiming at controlling the topology of the membrane protein within the lipid bilayer [46].

In addition to these practical considerations, there are some limitations to the model itself. In the case of Mistic, the protein had no noticeable influence on the location of the SAT and SOL boundaries (Fig. 7A). However, this finding does not necessarily hold true for other membrane proteins and other reconstitution protocols. For instance, when reconstituting the K^+ channel KcsA by titration of a micellar protein/detergent mixture with lipid vesicles [25], we observed drastic deviations of the experimental phase boundaries from those predicted on the basis of simple lipid/detergent mixtures, which was attributed to incomplete reconstitution and precipitation of the protein. Also, the model does not take into account micellar sphere-to-rod transitions [47], which are reflected in both solubilisation and reconstitution isotherms as additional, rather smooth transitions outside the coexistence range (Fig. 3), and nonideal mixing of lipid and detergent. For the system under investigation, considerable attractive interactions between the dipolar headgroups of LDAO and POPC might be expected. Furthermore, partitioning of CD into the micellar core could add to and thus complicate the partition equilibria underlying our model [48]. However, including such interactions into the model is beyond the scope of this contribution and, in the present case, seems of little relevance, as can be concluded from the close agreement of experimental and predicted data (Figs. 6B and 7A).

When all prerequisites for the model are fulfilled, a complete set of thermodynamic parameters as given in Table 1 for a new set of CD, lipid, and detergent can be established within a few days. A typical set of experiments comprises a demicellisation experiment to determine the CMC, three or more solubilisation and reconstitution experiments each to derive the phase diagram, and a CD/detergent binding experiment to derive the dissociation constant. Since the partition coefficient of the detergent between the aqueous and micellar phases can be extracted also from the phase diagram itself, the demicellisation experiment is not strictly required. Nevertheless, independent determination of the CMC helps in narrowing down the error margins of the other parameters derived from the phase diagram; however, since the CMCs of many detergents are available in the literature, the demicellisation experiment may be omitted even in such cases.

5. Conclusions

We have established and validated a model that accounts for all linked equilibria in ternary CD/lipid/detergent mixtures in order to predict changes in the aggregational state encountered in the course of CD-mediated reconstitution titrations, in particular, the onset and completion of reconstitution. The model can be adapted to other CD/lipid/detergent combinations using a set of tried-and-tested ITC protocols for determining thermodynamic parameters comprising the detergent's CMC, the lipid/detergent phase diagram, and the dissociation constant of the CD/detergent complex. On the basis of our model and the calorimetric approach outlined above, controlled sequestration of detergent upon addition of CD to an initially micellar mixture allows for highly reproducible and low-volume membrane-protein reconstitution, which enables the optimisation of key parameters such as the protein/lipid ratio and the rate of detergent removal and hence obviates cumbersome trial-and-error approaches. Moreover, CD-mediated reconstitution alleviates several disadvantages entailed by more conventional reconstitution methods and, as an addition or alternative to calorimetry, allows for spectroscopic monitoring of the reconstitution process. All equations and calculations underlying our model have been implemented in a Microsoft Excel worksheet, which is available from the authors upon request.

6. Theory

The following model describing linked equilibria in a ternary CD/lipid/detergent mixture is, to some extent, analogous to competitive binding models [49–51] and to the partitioning model for lipid/detergent mixtures [33], since it represents a combination of (i) pseudophase partitioning of detergent (D) among micellar (m), bilayer (b), and aqueous (aq) phases and of lipid (L) between micellar and bilayer phases and (ii) stoichiometric binding of detergent to CD (Fig. 1C). The notation applied throughout the following equations refers to molecular components (i.e., D, L, and CD) in subscripts and pseudophases (i.e., m, b, and aq) or inclusion complex (i.e., i) in superscripts.

6.1. Demicellisation

The partition coefficient for the transfer of detergent from the aqueous phase to the micellar phase, $P_D^{m/aq}$, is derived from the CMC of the detergent as

$$P_D^{m/aq} \equiv \frac{X_D^m}{X_D^{aq}} = \frac{c_D^{aq} + c_W}{c_D^{aq}} \approx \frac{c_W}{c_D^{aq}} = \frac{c_W}{CMC} \quad (1)$$

with $X_D^m = 1$ and X_D^{aq} denoting the mole fractions of detergent in the micellar and aqueous phases, respectively, and c_D^{aq} being the molar concentration of detergent monomers in the bulk aqueous phase. The latter is negligible in comparison with the much higher concentration of water (W), $c_W = 55.5$ M, and, in the absence of lipid, is equal to the CMC. The latter, in turn, is derived by fitting an ITC demicellisation isotherm using a generic sigmoidal function [32] of the form

$$Q(c_D) = \frac{A_1 - A_2}{1 + \exp\left(\frac{c_D - CMC}{\Delta c_D}\right)} + A_2 \quad (2)$$

with Q denoting the normalised heat of reaction and c_D the detergent concentration. A_1 and A_2 are linear functions describing the baselines in the pre- and post-transition regions, respectively, and Δc_D is a parameter determining the width of the transition region.

6.2. Lipid/detergent phase diagram

The other parameters describing pseudophase partitioning required by the model are obtained from the lipid/detergent phase diagram. The phase boundaries in the phase diagram are given by linear equations of the form

$$c_D^{SAT} = R_D^{b,SAT} c_L + c_D^{aq,SAT} \quad (3)$$

$$c_D^{SOL} = R_D^{m,SOL} c_L + c_D^{aq,SOL} \quad (4)$$

where c_D^{SAT} is the total detergent concentration required for bilayer saturation, c_D^{SOL} the total detergent concentration required for

complete solubilisation, and c_L the total lipid concentration. The slopes of the SAT and SOL boundaries reflect the molar ratios of detergent to lipid at bilayer saturation, $R_D^{b,SAT} \equiv c_D^{b,SAT}/c_L$, and complete solubilisation, $R_D^{m,SOL} \equiv c_D^{m,SOL}/c_L$, respectively. The concentrations of detergent in the aqueous phase, $c_D^{aq,SAT}$ and $c_D^{aq,SOL}$, correspond to the y-axis intercepts of the phase boundaries. According to Gibbs' phase rule, these concentrations must be identical [52], so that a common intercept $c_D^{aq^\circ} \equiv c_D^{aq,SAT} = c_D^{aq,SOL}$ for both phase boundaries can be defined. Since $c_D^{aq^\circ}$ refers to detergent monomers in equilibrium with mixed micelles and mixed bilayers, $c_D^{aq^\circ}$ is smaller than the CMC of the detergent, which refers to the equilibrium of detergent monomers with pure detergent micelles. From the slopes of the phase boundaries, the mole fractions of detergent in detergent-saturated bilayers and in lipid-saturated micelles can be determined as

$$X_D^{b,SAT} = \frac{R_D^{b,SAT}}{1 + R_D^{b,SAT}} \tag{5}$$

$$X_D^{m,SOL} = \frac{R_D^{m,SOL}}{1 + R_D^{m,SOL}} \tag{6}$$

The parameters describing pseudophase partitioning include the partition coefficients of lipid between the bilayer and micellar phases, $P_L^{b/m}$, and of detergent between the bilayer and micellar phases, $P_D^{b/m}$, as well as between the bilayer and aqueous phases, $P_D^{b/aq}$. These partition coefficients are given by the mole fractions of lipid and detergent in the pseudophases according to

$$P_L^{b/m} \equiv \frac{X_L^b}{X_L^m} = \frac{1 - X_D^b}{1 - X_D^m} = \frac{c_L^b\left(c_L^m + c_D^m\right)}{c_L^m\left(c_L^b + c_D^b\right)} \tag{7}$$

$$P_D^{b/m} \equiv \frac{X_D^b}{X_D^m} = \frac{c_D^b\left(c_L^m + c_D^m\right)}{c_D^m\left(c_L^b + c_D^b\right)} \tag{8}$$

$$P_D^{b/aq} \equiv \frac{X_D^b}{X_D^{aq}} = \frac{c_D^b\left(c_D^{aq} + c_W\right)}{c_D^{aq}\left(c_L^b + c_D^b\right)} \approx \frac{c_D^b c_W}{c_D^{aq}\left(c_L^b + c_D^b\right)} \tag{9}$$

6.3. Stoichiometric binding of detergent to CD

In addition to the parameters for pseudophase partitioning, the model requires the dissociation constant, $K_D^{i/aq}$, describing 1:1 binding of detergent to CD according to

$$K_D^{i/aq} \equiv \frac{c_D^{aq} c_{CD}^{aq}}{c_D^i} \tag{10}$$

Here, c_D^i and c_{CD}^{aq} stand for the molar concentrations of detergent in the inclusion complex and of unbound CD in the aqueous phase, respectively. Substitution of $c_{CD}^{aq} = c_{CD} - c_D^i$ into Eq. (10) then yields

$$c_D^i = \frac{c_D^{aq}}{c_D^{aq} + K_D^{i/aq}} c_{CD} \tag{11}$$

6.4. Combination of linked equilibria

Mass conservation gives the total detergent concentration as

$$c_D = c_D^m + c_D^b + c_D^{aq} + c_D^i \tag{12}$$

and the total lipid concentration as

$$c_L = c_L^m + c_L^b \tag{13}$$

6.4.1. Coexistence range

Within the coexistence range, combining these two equations with the definitions of $R_D^{b,SAT}$ and $R_D^{m,SOL}$ and with the equality $c_D^{aq} = c_D^{aq^\circ}$ yields the concentration of lipid in the micellar phase as

$$c_L^m = \frac{c_D - c_D^{aq^\circ} - c_D^i - R_D^{b,SAT} c_L}{R_D^{m,SOL} - R_D^{b,SAT}} \tag{14}$$

where c_D^i is provided by Eq. (11) and $c_D^{aq^\circ}$ is given by combining Eqs. (1) and (6) as

$$c_D^{aq^\circ} = CMC \cdot X_D^{m,SOL} = CMC \cdot \frac{R_D^{m,SOL}}{1 + R_D^{m,SOL}} \tag{15}$$

According to the definition of $R_D^{m,SOL}$, the concentration of detergent in the micellar phase then simply is

$$c_D^m = R_D^{m,SOL} c_L^m \tag{16}$$

6.4.2. Micellar range

Within the micellar range, $c_L^m = c_L$, insertion of which into Eq. (10) with $X_D^{m,SOL} = c_D^m/(c_D^m + c_L^m)$ and $X_D^{aq} = c_D^{aq}/(c_D^{aq} + c_W)$ furnishes

$$c_D^m = \frac{c_D^{aq} P_D^{m/aq}}{c_W - c_D^{aq} P_D^{m/aq}} c_L \tag{17}$$

Combination with Eqs. (11) and (12) then results in

$$c_D^{aq} = c_D - \frac{c_D^{aq} P_D^{m/aq}}{c_W - c_D^{aq} P_D^{m/aq}} c_L - \frac{c_{CD} c_D^{aq}}{c_D^{aq} + K_D^{i/aq}} \tag{18}$$

which is rearranged into a cubic equation of the form

$$c_D^{aq^3} + p c_D^{aq^2} + q c_D^{aq} + r = 0 \tag{19}$$

with coefficients

$$p = P_D^{m/aq}\left(K_D^{i/aq} + c_{CD} - c_D - c_L\right) - c_W \tag{20}$$

$$q = c_W\left(c_D - c_{CD} - K_D^{i/aq}\right) - P_D^{m/aq} K_D^{i/aq}(c_D - c_L) \tag{21}$$

$$r = K_D^{i/aq} c_D c_W \tag{22}$$

The only physically meaningful solution of Eq. (19) is

$$c_D^{aq} = \frac{2}{3}\sqrt{p^2 - 3q}\cos\left(\frac{2\pi - \theta}{3}\right) - \frac{p}{3} \tag{23}$$

where

$$\theta = \arccos\frac{-2p^3 + 9pq - 27r}{2\sqrt{(p^2 - 3q)^3}} \tag{24}$$

6.4.3. Bilayer range

Within the bilayer range, $c_L^b = c_L$, insertion of which into Eq. (9) gives

$$c_D^b = \frac{c_D^{aq} P_D^{b/aq}}{c_W - c_D^{aq} P_D^{b/aq}} c_L \tag{25}$$

which is analogous to Eq. (17). Applying the same substitutions and rearrangements as used above for the micellar range, one arrives at a cubic equation with coefficients analogous to those in Eqs. (20)–(22), the only difference being that $P_D^{b/aq}$ now takes the place of $P_D^{m/aq}$.

6.4.4. Speciation plot

On the basis of this set of equations, it is possible to calculate the concentrations of all components in each pseudophase for any CD/lipid/detergent mixture (e.g., Fig. 6C) given that the CMC, $R_D^{b,SAT}$, $R_D^{m,SOL}$, and $K_D^{i/aq}$ values are known. Additionally, since positive and, thus, physically meaningful detergent and lipid concentrations for both the micellar and the bilayer phases are obtained only within the coexistence range, application of the above equations to all injections of a reconstitution titration identifies the SAT and SOL phase boundaries by a change in sign of c_D^m and c_L^m at the SAT boundary and of c_D^b and c_L^b at the SOL boundary.

Acknowledgements

We thank Georg Krainer (B Cube Dresden) for constructive comments on the manuscript. This work was supported by a scholarship from the German National Academic Foundation (to M.T.) and by the International Research Training Group 1830 funded by the Deutsche Forschungsgemeinschaft (DFG).

References

[1] J.P. Overington, B. Al Lazikani, A.L. Hopkins, Nat. Rev. Drug Discov. 5 (2006) 993–996.
[2] E. Racker, Methods Enzymol. 55 (1979) 699–711.
[3] J.L. Rigaud, D. Lévy, Methods Enzymol. 372 (2003) 65–86.
[4] H. Heerklotz, G. Lantzsch, H. Binder, G. Klose, A. Blume, Chem. Phys. Lett. 235 (1995) 517–520.
[5] H. Heerklotz, A.D. Tsamaloukas, S. Keller, Nat. Protoc. 4 (2009) 686–697.
[6] D. Lichtenberg, Biochim. Biophys. Acta 821 (1985) 470–478.
[7] J. Rigaud, M. Chami, O. Lambert, D. Lévy, J. Ranck, Biochim. Biophys. Acta 1508 (2000) 112–128.
[8] M. Ollivon, S. Lesieur, C. Grabielle-Madelmont, M. Paternostre, Biochim. Biophys. Acta 1508 (2000) 34–50.
[9] S. Keller, H. Heerklotz, A. Blume, J. Am. Chem. Soc. 128 (2006) 1279–1286.
[10] D.D. Lasic, Biochem. J. 256 (1988) 1–11.
[11] W. Jiskoot, T. Teerlink, E.C. Beuvery, D.J. Crommelin, Pharm. Week. Sci. 8 (1986) 259–265.
[12] P. Schurtenberger, N. Mazer, S. Waldvogel, W. Känzig, Biochim. Biophys. Acta 775 (1984) 111–114.
[13] E. Racker, B. Violand, S. O'Neal, M. Alfonzo, J. Telford, Arch. Biochem. Biophys. 198 (1979) 470–477.
[14] A. Engel et al., J. Struct. Biol. 109 (1992) 219–234.
[15] M.H. Milsmann, R.A. Schwendener, H.G. Weder, Biochim. Biophys. Acta 512 (1978) 147–155.
[16] T.M. Allen, A.Y. Romans, H. Kercret, J.P. Segrest, Biochim. Biophys. Acta 601 (1980) 328–342.
[17] T. Ruysschaert, A. Marque, J.L. Duteyrat, S. Lesieur, BMC Biotechnol. 5 (2005) 1–13.
[18] D. Lévy, A. Bluzat, M. Seigneuret, J.L. Rigaud, Biochim. Biophys. Acta 1025 (1990) 179–190.
[19] J.L. Rigaud et al., J. Struct. Biol. 118 (1997) 226–235.
[20] J.L. Rigaud, D. Lévy, G. Mosser, O. Lambert, Eur. Biophys. J. 27 (1998) 305–319.
[21] W.J. DeGrip, J. Vanoostrum, P.H.M. Bovee-Geurts, Biochem. J. 330 (1998) 667–674.
[22] S. Mahammad, I. Parmryd, Methods Mol. Biol. 1232 (2015) 91–102.
[23] G.A. Signorell, T.C. Kaufmann, W. Kukulski, A. Engel, H.W. Rémigy, J. Struct. Biol. 157 (2007) 321–328.
[24] M.V. Rekharsky, Y. Inoue, Chem. Rev. 98 (1998) 1875–1917.
[25] N. Jahnke et al., Anal. Chem. 86 (2014) 920–927.
[26] S. Paula, W. Süs, J. Tuchtenhagen, A. Blume, J. Phys. Chem. 99 (1995) 11742–11751.
[27] T. Wiseman, S. Williston, J.F. Brandts, L.N. Lin, Anal. Biochem. 179 (1989) 131–137.
[28] T.P. Roosild et al., Science 307 (2005) 1317–1321.
[29] J. Broecker, S. Fiedler, K. Gimpl, S. Keller, J. Am. Chem. Soc. 136 (2014) 13761–13768.
[30] D.K. Debnath, R.V. Basaiawmoit, K.L. Nielsen, D.E. Otzen, Protein Eng. Des. Sel. 24 (2011) 89–97.
[31] S. Keller et al., Anal. Chem. 84 (2012) 5066–5073.
[32] J. Broecker, S. Keller, Langmuir 29 (2013) 8502–8510.
[33] O.O. Krylova, N. Jahnke, S. Keller, Biophys. Chem. 150 (2010) 105–111.
[34] J.C. Houtman et al., Protein Sci. 16 (2007) 30–42.
[35] G. Kemmer, S. Keller, Nat. Protoc. 5 (2010) 267–281.
[36] P.A. Hassan, S. Rana, and G. Verma, Langmuir , in press (2014).
[37] T. Jacso et al., J. Am. Chem. Soc. 135 (2013) 18884–18891.
[38] H. Heerklotz, G. Lantzsch, H. Binder, G. Klose, A. Blume, J. Phys. Chem. 100 (1996) 6764–6774.
[39] S. Keller, H. Heerklotz, N. Jahnke, A. Blume, Biophys. J. 90 (2006) 4509–4521.
[40] Y. Imaishi, R. Kakehashi, T. Nezu, H. Maeda, J. Colloid Interface Sci. 197 (1998) 309–316.
[41] P. Strop, A.T. Brunger, Protein Sci. 14 (2005) 2207–2211.
[42] S.K. Mehta, K.K. Bhasin, S. Dham, M.L. Singla, J. Colloid Interface Sci. 321 (2008) 442–451.
[43] A.D. Tsamaloukas, S. Keller, H. Heerklotz, Nat. Protoc. 2 (2007) 695–704.
[44] Z. Huang, E. London, Langmuir 29 (2013) 14631–14638.
[45] D.D. Lasic, F.J. Martin, J.M. Neugebauer, J.P. Kratohvil, J. Colloid Interface Sci. 133 (1989) 539–544.
[46] A. Helenius, M. Sarvas, K. Simons, Eur. J. Biochem. 116 (1981) 27–35.
[47] H. Heerklotz, Q. Rev. Biophys. 41 (2008) 205–264.
[48] M. Tsianou, A.I. Fajalia, Langmuir 30 (2014) 13754–13764.
[49] G. Krainer, J. Broecker, C. Vargas, J. Fanghänel, S. Keller, Anal. Chem. 84 (2012) 10715–10722.
[50] G. Krainer and S. Keller, Methods 76 (2015) 116–123.
[51] Z.X. Wang, FEBS Lett. 360 (1995) 111–114.
[52] D. Lichtenberg, R.J. Robson, E.A. Dennis, Biochim. Biophys. Acta 737 (1983) 285–304.